“Development of Tin Compounds with Nano-Micro Hierarchical Structures for Thermoelectrics.”

A Thesis

Submitted to
Indian Institute of Science Education and Research Pune
In partial fulfilment of the requirements for the
BS-MS Dual Degree Programme

By,

Chinmay Manisha Ajay Timane

Indian Institute of Science Education and Research Pune
Dr. Homi Bhabha Road,
Pashan, Pune 411008, INDIA.

April 2018

Supervisor: Prof. Sulabha K. Kulkarni

Certificate

This is to certify that this dissertation entitled "**Development of Tin Compounds with Nano-Micro Hierarchical Structures for Thermoelectrics***"* towards the partial fulfilment of the BS-MS dual degree programme at the Indian Institute of Science Education and Research Pune represents study/work carried out by Mr.Chinmay Timane at IISER Pune under the supervision of Prof. Sulabha K. Kulkarni, INSA Senior Scientist, Centre for Materials for Electronics Technology (CMET), during the academic year 2017-2018.

Student Sign

Supervisor Sign

Committee:

Name of Supervisor - *Prof. Sulabha K. Kulkarni*

Name of TAC – *Dr. Surjit Singh.*

रोज दुपारी पडलेल्या स्वप्नांना समर्पित.

Declaration

I hereby declare that the matter embodied in the report entitled "**Development of Tin Compounds with Nano-Micro Hierarchical Structures for Thermoelectrics**" are the results of the work carried out by me at the Department of Physics, IISER Pune, under the supervision of **Prof. Sulabha K. Kulkarni** and the same has not been submitted elsewhere for any other degree.

Supervisor Sign

Student Sign

Acknowledgements

I Thank Prof. Sulabha Kulkarni for supervising the project work throughout the year. I thank Dr. Surjit Sing for timely advice about project and for allowing me to use his lab for project related works. I thank Mr. Saurabh Kumar (Ph.D. student, Dr. Surjit Sing lab) for assisting me in sintering of pellet. I thank Anu (BS-MS fifth year, Dr.J.K. lab) for helping in thermal analysis of material. I thank Mr. Anil and Mr. Yatish for helping in FESEM imaging and EDAX analysis. I thank IISER Pune for providing XRD facility. I thank Dean physics dept. IISER Pune for allowing me to work in the common wet lab. In the end, thanks to my family and friends for being supportive.

Table of Contents

List of Figures

List of Tables

1. Abstract

Thermoelectric materials convert heat energy into electric energy. Thermoelectric performance of such materials needs to be enhanced in order to achieve higher conversion efficiency. Strategies like introducing point defects in the material, having nano-inclusions can be used to enhance the thermoelectric performance. In this project, we have focused our study on SnS material. We could synthesize SnS using hydrothermal approach by two different methods. SnS synthesized by one method has large particle size of few micrometers, whereas another method gives SnS at nanoscale. We shall use the nano-micro composition strategy to observe any changes in the thermoelectric performance of SnS.

2. Introduction

Thermoelectric effect was first observed by Thomas Seebeck in 1821. He observed a current flow in a loop formed by jointing two different metals, whose junctions were kept at different temperatures. The same phenomenon can be observed in semiconductors also. An arrangement of two semiconductors, p-type and n-type junctioned together at both ends (**figure a**) where one junction was kept at hotter temperature and another junction at cooler temperature and thus forcing charge carriers to migrate from hotter side to cooler side generating unidirectional current in the circuit. This generation of electric current due to the temperature difference applied was named as 'Seebeck effect' and used for the purpose of power generation. Conversely, when an electric voltage was applied across the two semiconductor legs (**figure b**) holes in p-type tend to move towards negative terminal of battery and electrons in n-type tend to move towards positive terminal of battery, thus the resultant movements of charge carriers is towards that junction which is connected to the battery. The voltage-driven accumulation of charge carriers at one junction causes that junction to heat up and continuos removal of heat from that junction lowers the temperature of other junction. This voltage driven temperature difference generation is named as 'Peltier effect' and used for the purpose of refrigeration.

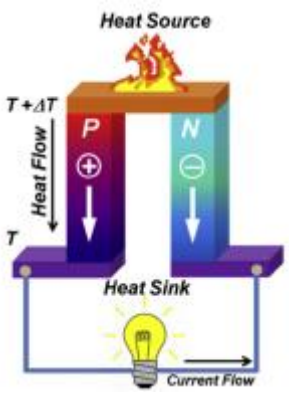

Figure (a)

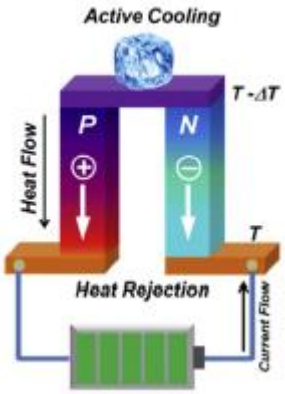

Figure (b)

Image sources: X. Zhang, L.-D. Zhao / *J. Mater.* **1,** 92–105 (2015).

figure (a) *is schematic representation of Seebeck effect and* ***figure (b)*** *is schematic representation of Peltier effect.*

The thermoelectric performance of material is defined by a dimensionless quantity called figure of merit, ZT, which is given by the expression $ZT = (\alpha^2\sigma/K)T$, where α is the Seebeck coefficient of material, σ is electrical conductivity, K is the thermal conductivity and T is temperature. It can be clearly observed from the expression that in order to enhance ZT, the material should have higher electrical conductivity but at the same time a low thermal conductivity. Following expressions show the relationship between electrical and thermal conductivity-

$$\sigma = \frac{ne^2\tau}{m^*} \quad \text{and} \quad K = K_{lattice} + K_{electronic} = K_{lattice} + L\sigma T$$

where n is carrier concentration, e is electronic charge, τ is relaxation time, m* is effective mass of electron, $K_{lattice}$ is lattice contribution to total thermal conductivity and $K_{electronic}$ is electronic contribution to total thermal conductivity, L is Lorentz number, T is temperature.

Hence, any attempt to increase electrical conductivity will also increase thermal conductivity as electrical conductivity is directly related to thermal conductivity through the electronic contribution in thermal conductivity. Thus it is convincing to focus on lattice contribution of thermal conductivity and minimize it in order to increase the σ/K ratio.

Heat transfer in lattice takes place mainly because of phonon propagation. Phonons are nothing but the collective vibration of all atoms/ions in a lattice that propagates through it with single frequency. Phonons with different wavelengths can be present in lattice. Thus to minimize the heat transfer in the material phonon scattering plays an essential role. Introducing point defects, having nano-inclusions, grain boundaries are some of the ways for phonon scattering to occur[1]. In this project a strategy where a mixture of nano-sized material and same material of fairly large particle size will be examined for thermoelectric behavior.

Several materials have been investigated for their thermoelectric figure of merit value. Most of these materials were containing heavy, toxic, less abundant elements[2]. SnSe is one among them; it has shown ultralow thermal conductivity and high thermoelectric performance due to its unique layered structure type[3]. SnS which belongs to the same family of compounds also resembles the SnSe structure type[4].

Also, the low toxicity and our green approach of synthesis of SnS make it a perfect candidate to be investigated for thermoelectrics.

3. Methods

SnS is synthesized using hydrothermal approach by two different methods.

3.1 Hydrothermal Synthesis

A method where chemical precursors are dissolved in water in a vessel which is mostly a Teflon liner. This Teflon liner is closed tightly and then placed in a strong metal container (usually of stainless steel) which is covered and tightened using nuts and bolts. The metal container is strong enough to withhold a very high pressure. It should be tightened properly so no water vapor from inside vessel leak. A key feature of Hydrothermal method is that it can carry out reactions at high temperature and high pressure of water vapors inside (temperature up to 300^0C and pressure around 100 bars or even more high depending upon strength of autoclave). This method enables a large scale production of nano/micro sized materials with high uniformity in size and shapes of particles. Another method which follows the same principle but uses a solvent other than water for the reaction is called **solvothermal** method.

3.2 Synthesis methods

3.2.1 Method 1

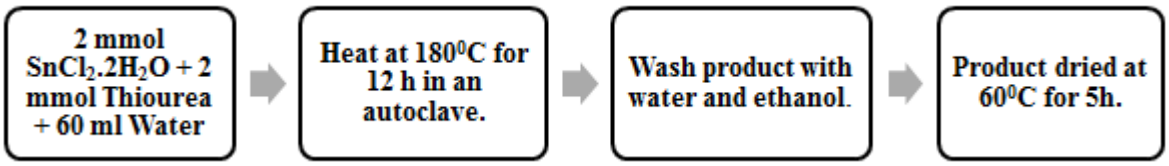

Figure (c): Schematic of method 1 synthesis

2 mmol of $SnCl_2.2H_2O$ was dissolved in 25 ml of distilled water. Similarly, 2 mmol of Thiourea was dissolved in 25 ml distilled water separately. The solutions were transferred to 80 ml Teflon liner and the final volume of reaction mixture was made up to 60 ml by addition of 10 ml distilled water. The autoclave was then placed in a hot air oven at 180^0C for 12 hours. After 12 hours, the autoclave was allowed to cool down to room temperature. The product was settled down as dark grey particles which were separated from the solution by decanting the liquid out. Then the product was washed with distilled water then with absolute ethanol several times by centrifugation. The washed product was kept in a vacuum oven at 60^0C for 5 hours to dry and finally collected as powder.

3.2.2 Method 2

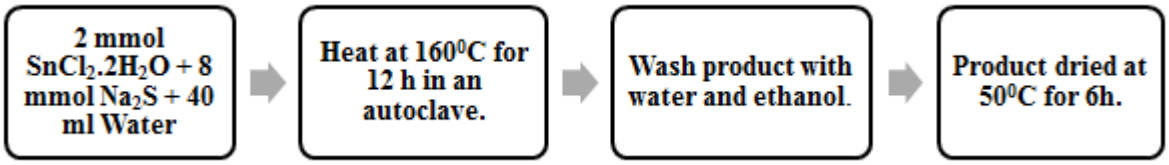

Figure (d): Schematic of method 2 synthesis

2 mmol of $SnCl_2.2H_2O$ was dissolved in 20 ml distilled water and 8 mmol of Na_2S was dissolved in 20 ml distilled water separately. The $SnCl_2$ solution was added dropwise to the Na_2S solution in the 80 ml Teflon liner. Mixture turns dark brown upon addition of $SnCl_2$ solution. The autoclave was then placed in a hot air oven at 160^0C for 12 hours. After 12 hours, the autoclave was allowed to cool down to room temperature. The product was separated from the solution and was washed with distilled water then with absolute ethanol several times by centrifugation. The washed product was then kept into the vacuum oven at 50^0C for 6h to dry and finally collected as powder.

The products which were obtained as powder by method 1 and method 2 were characterized by powder X-ray diffraction, FESEM and EDAX analysis.

3.3 Characterising Techniques

3.3.1 FESEM and EDAX

The underlying principle of FESEM (Field Emission Scanning Electron Microscopy) is same as that of optical microscopy. It uses the wave-particle duality of matter. In optical microscopy, electromagnetic waves from incident light are scattered from sample and then collected by placing lenses for imaging. Here in FESEM electrons are incident on sample and those which are backscattered by sample are collected by placing electrostatic or magnetic lenses. But unlike light, electrons can interact with material by ionization (if sample is non conducting), by producing secondary electrons (incident electrons eject electrons from sample), X-rays, visible light and thus affecting the resolution/imaging in some cases. FESEM is useful technique for imaging surfaces of particles of nano/micro size.

As mentioned above, when the secondary electrons are ejected from sample atom after the collision with incident electrons, a vacancy is created in the respective energy level. So an electron in the upper energy level releases energy equal to the energy difference of those levels to fill that vacancy. Released energy is in form of X-rays which are characteristic. They are detected by the detector which helps to identify element and also gives quantitative estimate of its abundance in the sample. This technique is called Energy Dispersive Analysis of X-rays (EDAX)

3.3.2 Powder X-ray diffraction

X-ray diffraction technique is used to understand crystal structure of material. X-rays are scattered in all directions by periodically arranged atoms/ions/molecules in the crystal because the wavelength of X-rays is comparable with the interatomic distances. But only those scattered rays that satisfy Bragg's condition (which is specific to each atomic plane) are detected as peaks in XRD. Powder sample has a random distribution of orientation of all crystallites, thus exposing various planes to the incident beam of X-Rays. Atomic planes show up in XRD pattern as sharp lines (broad in case of nano materials) with certain intensity that depends upon orientation

of atoms, nature of atoms and position of atoms in lattice. One can solve, confirm the material crystal structure by comparing its XRD pattern with the database of reported materials. Information such as unit cell parameters, inter-planer distances can be obtained from XRD pattern.

3.3.3 Thermogravimetric Analysis (TGA)

Thermogravimetric analysis records change in the weight of sample as a function of temperature. It is helpful to understand the thermal behaviour of a given material. Physical or chemical changes like vaporization of material, oxidation of material, decomposition etc. are reflected through the changes in weight of sample which are recorded.

3.3.4 Differential Scanning Calorimetry (DSC)

Differential Scanning Calorimetry records calorimetric changes in material by scanning in several cycles of heating and cooling. Heat flow is recorded as a function of temperature. So calorimetric events like melting, freezing, crystallization etc. are recorded as peaks or valleys (depending on the thermodynamics of the event) in the thermogram.

4. Results and discussion

4.1 Product Characterization.

4.1.1 Method 1 product characterization

The product was confirmed to be SnS by comparing its XRD pattern with SnS JCPDS 00-014-0620 and EDAX values which show stoichiometric Tin to sulfur ratio to be almost 1:1. Most particles were having plate-like morphology.

FESEM Images

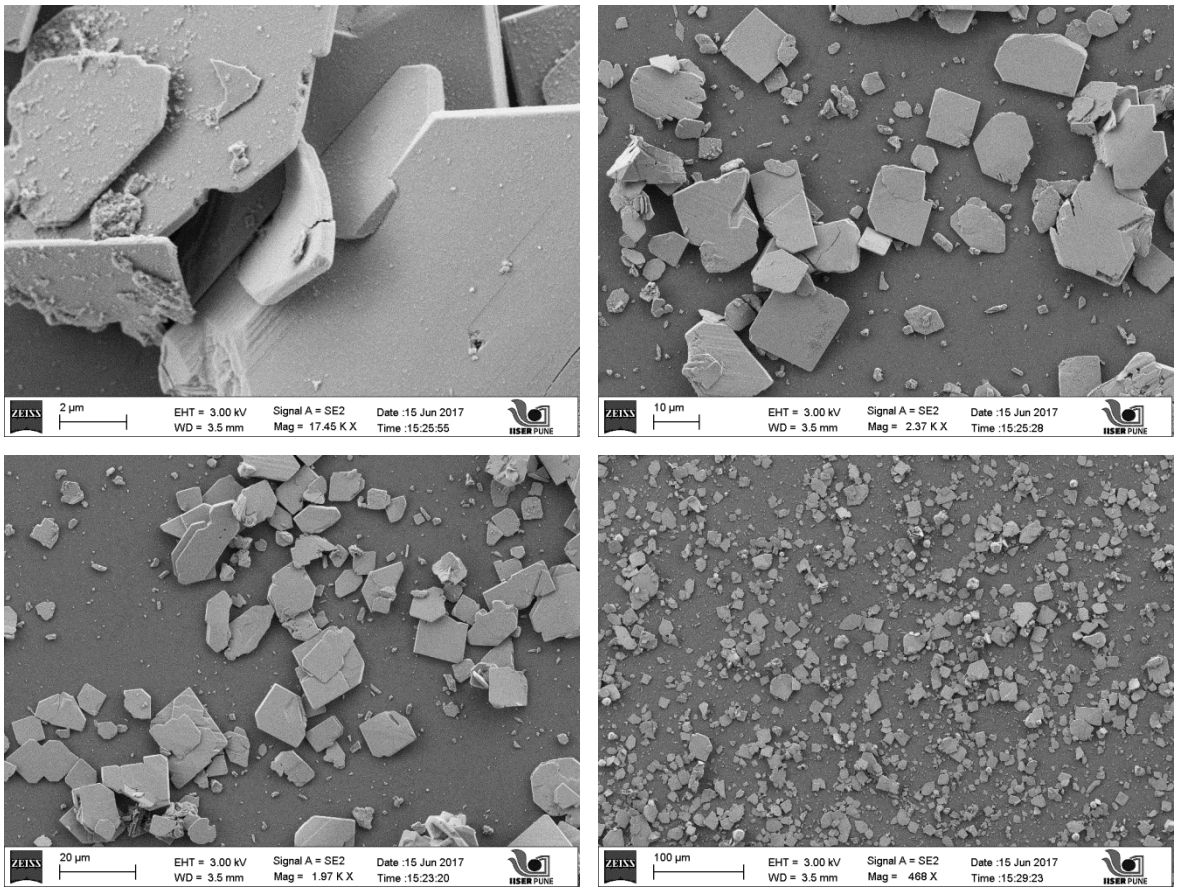

Figure 1: FESEM images of product obtained by method 1 @180^{0}C, 12h.

EDAX analysis

Element	Weight%	Atomic%
S K	21.54	50.40
Sn L	78.46	49.60
Totals	100.00	

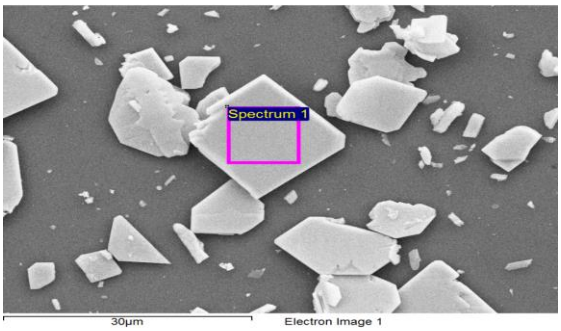

Figure 2: EDAX analysis of product synthesized by method 1.

Powder x-ray diffraction:

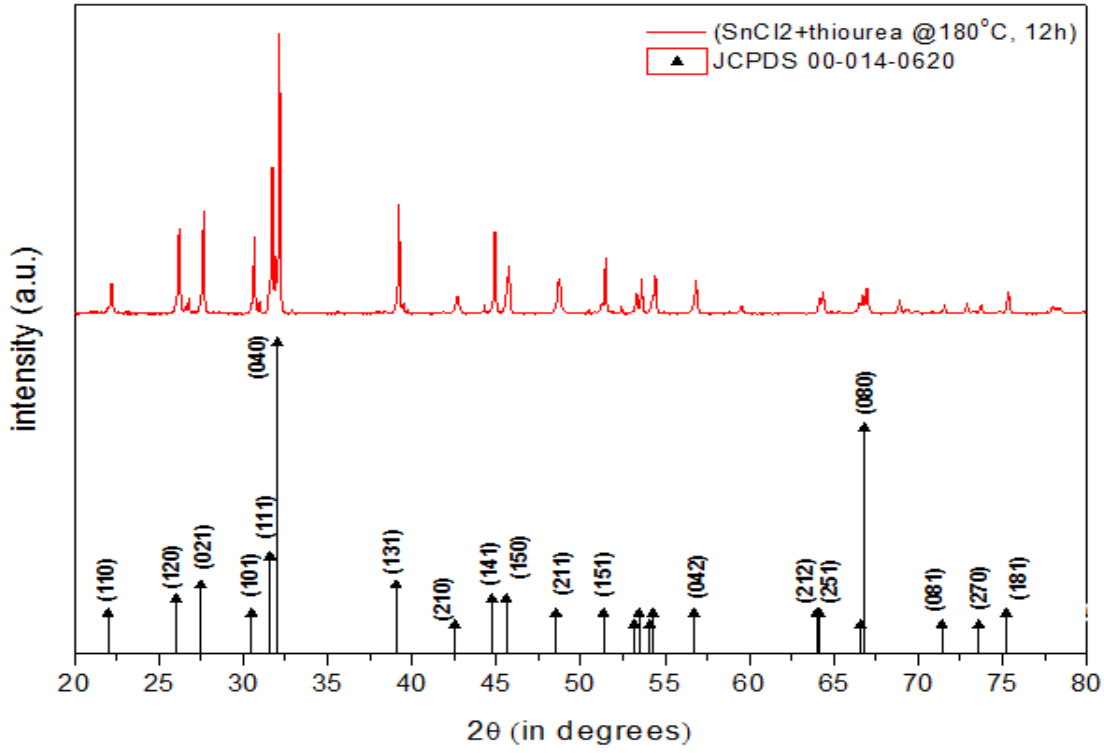

Figure 3: An XRD pattern of product obtained by method 1 @180^{0}C, 12h and compared with SnS JCPDS 00-014-0620.

4.1.2 method 2 product characterization

A mixture of three major morphologies were observed under FESEM – rods, plates and nano-sized flakes. Plates and rods were almost 1:1 in Sn:S ratio but nanoflakes were quite Tin rich. No JCPDS matched with XRD pattern of this product.

FESEM Images:

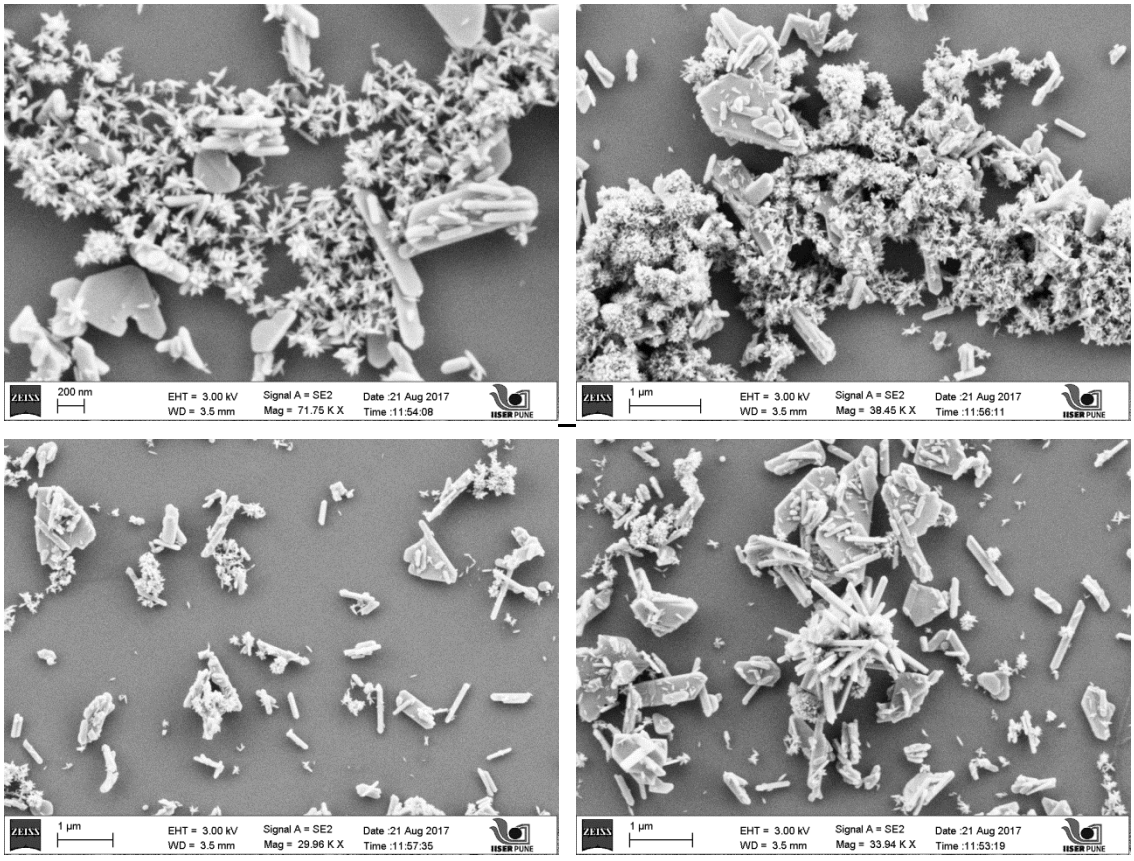

Figure 4: FESEM images of product obtained by method 2 @160^{0}C, 12h.

EDAX Analysis:

flakes	Weight%	Atomic%
S K	5.65	18.16
Sn L	94.35	81.84
Totals	100.00	

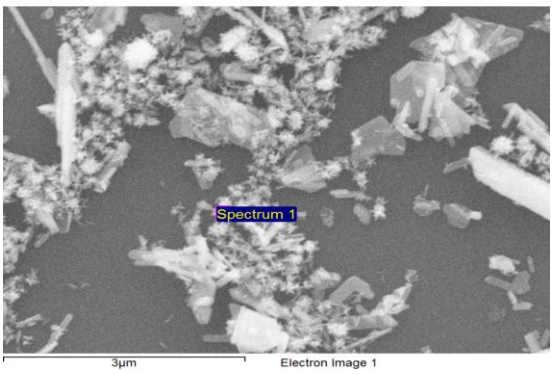

Plate	Weight%	Atomic%
S K	21.15	49.82
Sn L	78.85	50.18
Totals	100.00	

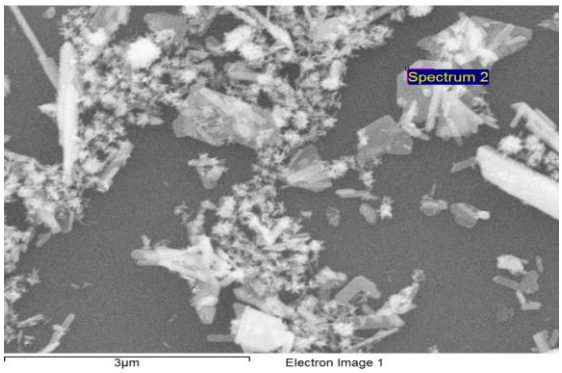

Rod	Weight%	Atomic%
S K	19.10	46.63
Sn L	80.90	53.37
Totals	100.00	

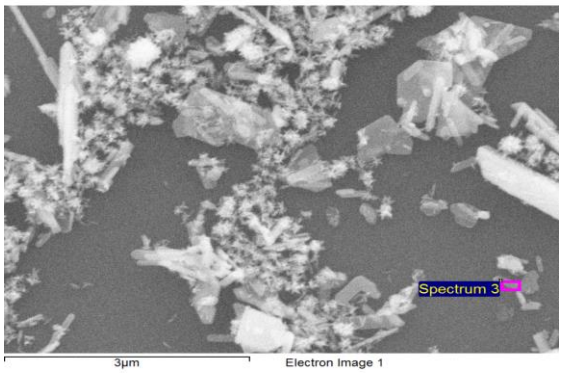

Figure 5: EDAX analysis of each major morphology of product synthesized by method 2.

Powder X-ray diffraction

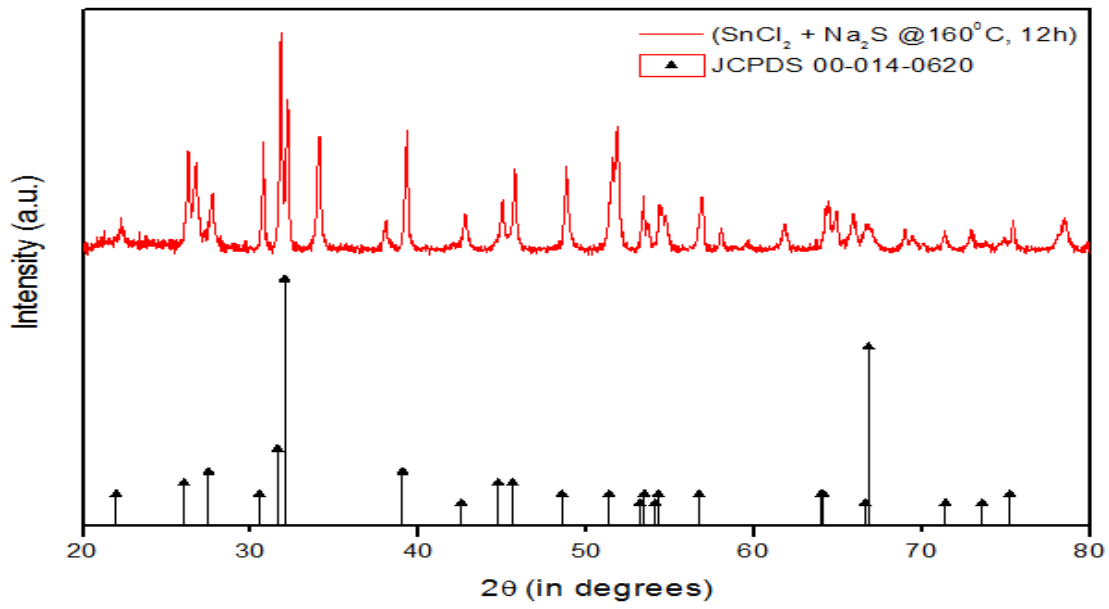

Figure 6: An XRD pattern of product obtained by method 2 @160^{0}C, 12h and compared with SnS JCPDS 00-014-0620.

4.2 Optimisation of reactions

After performing initial attempts to synthesize SnS by both methods, it was observed after characterizing that method 1 yielded SnS plates as major morphology whereas method 2 yielded rods, plates and nanoflakes altogether where rods and plates were almost 1:1 in Tin to sulfur ratio but nanoflakes were highly rich in Tin content.

Having checked the feasibility of formation of SnS by hydrothermal route with no additives, we decided to optimize the above method 1 and method 2 in both temperature and time domain. So to optimize both synthetic methods (method 1 and method 2) a series of syntheses were performed where in one case reaction time was kept constant (i.e.12 h for both methods) and the reaction temperature was varied. In another case, the reaction temperature was kept constant (180^0C for method 1 and 120^0C for method 2) and time of reaction was varied.

4.2.1 Method 1 optimization

In case of Method 1 where thiourea was used as the sulfur source, morphological changes and an increase in Tin percentage were observed with decrease in reaction temperature (figure 7 and Table 1). However, XRD patterns do not show any significant changes in the phases of these materials which were synthesized at different temperatures (figure 8). In another case where reaction temperature was kept constant and reaction time was varied, no significant changes were observed in the morphology of particles, atomic percentages of Tin, Sulfur and their X-Ray diffraction patterns (Figure 9, 10 and Table 2). Meanwhile, XRD patterns and EDAX values of atomic percentages assure the formation of Tin Sulfide (SnS) by method 1.

4.2.1.1 Temperature variation

FESEM Analyis:

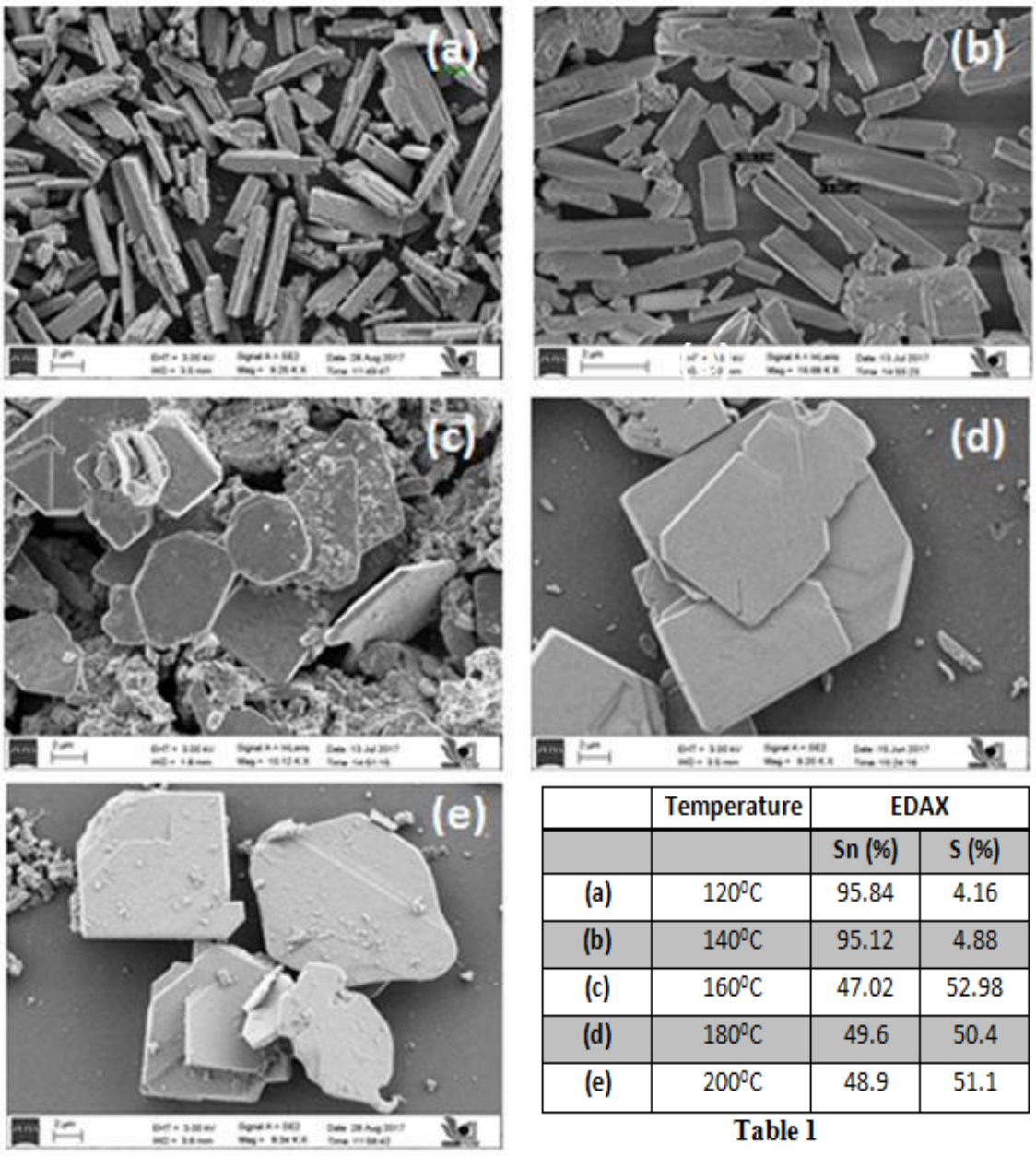

	Temperature	EDAX	
		Sn (%)	S (%)
(a)	120^{0}C	95.84	4.16
(b)	140^{0}C	95.12	4.88
(c)	160^{0}C	47.02	52.98
(d)	180^{0}C	49.6	50.4
(e)	200^{0}C	48.9	51.1

Table 1

Figure 7: FESEM images (a-e) of major morphologies obtained by method 1 with reaction time fixed for 12 hours and reaction temperature at (a) 120^{0}C, (b) 140^{0}C, (c) 160^{0}C, (d) 180^{0}C, (e) 200^{0}C. Whereas ***Table 1*** shows Tin, Sulfur percentages of particles from EDAX analysis.

XRD comparison:

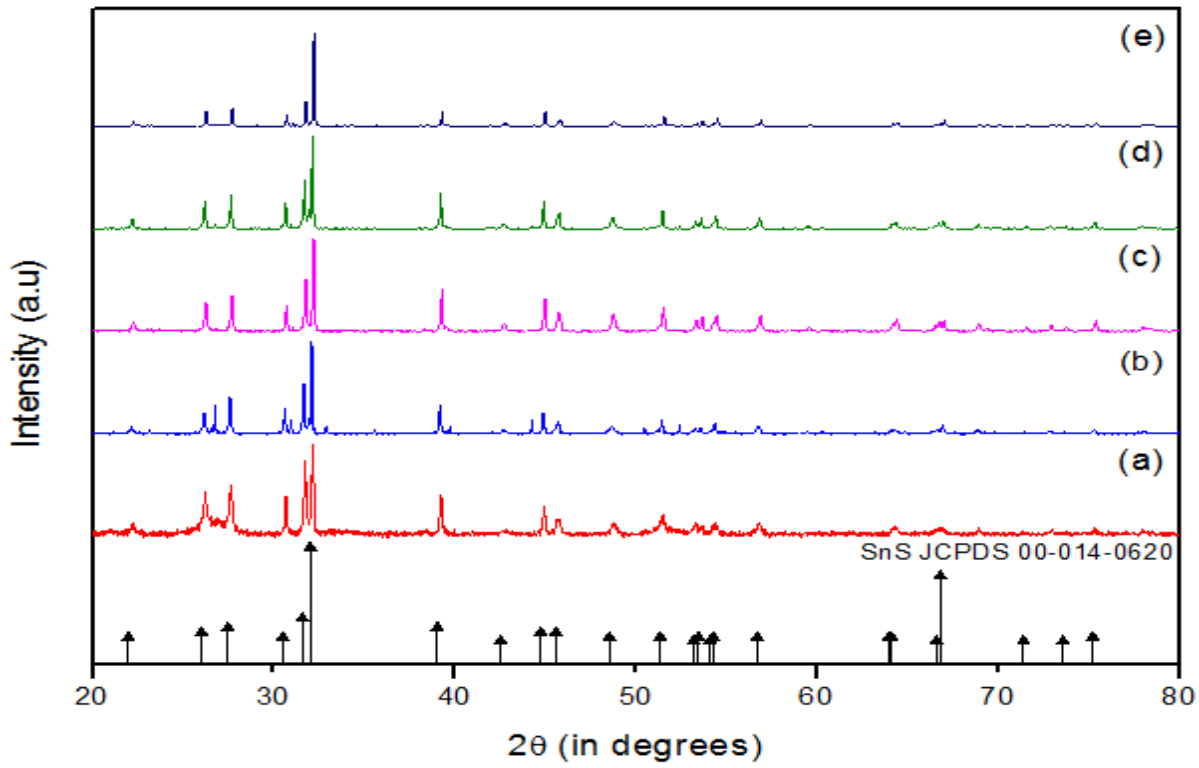

Figure 8 **:** comparison of XRD patterns of materials synthesized by method 1 at different temperatures for 12 hours; (a) at 120^0C, (b) at 140^0C, (c) at 160^0C, (d) at 180^0C, (e) at 200^0C.

Figure 7 clearly shows changes in morphology of particles from rectangular rods to plates as reaction temperature is increased. EDAX data, Table 1, shows that Tin content is increasing with decreasing reaction temperature. The rectangular rods have around 95% Sn and 5% S whereas plates are mostly 1:1 in Sn to S ratio. However, these changes in elemental ratios and morphology do not agree with XRD trend. XRD patterns of all materials are almost the same irrespective of the reaction temperature.

4.2.1.2 Time Variation

FESEM analysis:

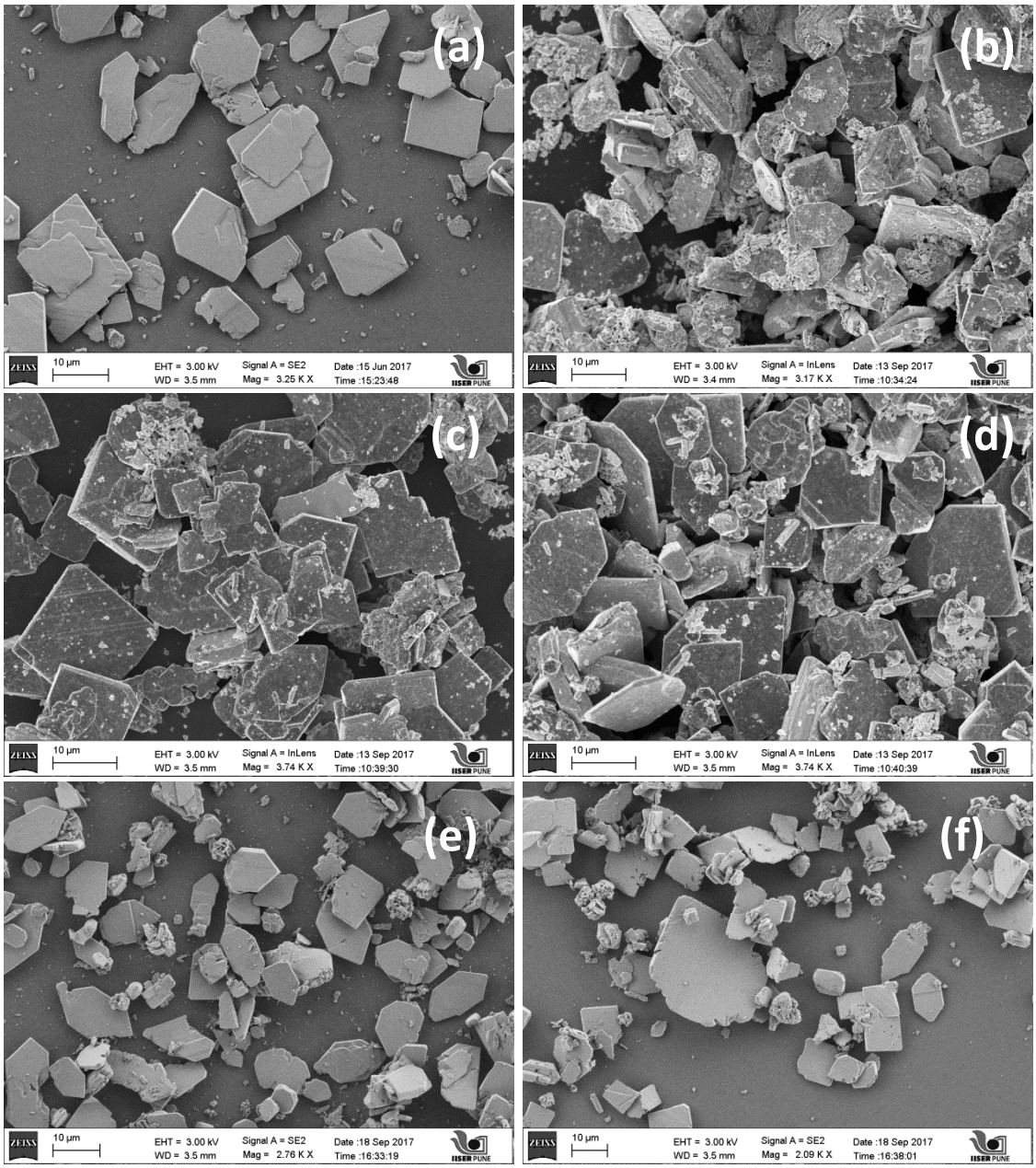

	Time	EDAX	
		Sn (%)	S(%)
(a)	12h	49.63	50.37
(b)	14h	49.42	50.58
(c)	16h	47.97	52.03
(d)	18h	49.83	50.17
(e)	20h	49	51
(f)	24h	49.23	50.77

Table 2

Figure 9 : FESEM images (a-f) of major marphologies obtained by method 1, performed at 180^0C with reaction time varying as: (a) 12h, (b) 14h, (c) 16h, (d) 18h, (e) 20h, (f) 24h**;** whereas ***Table 2*** shows Tin, Sulfur percentages of particles from EDAX analysis.

XRD comparison:

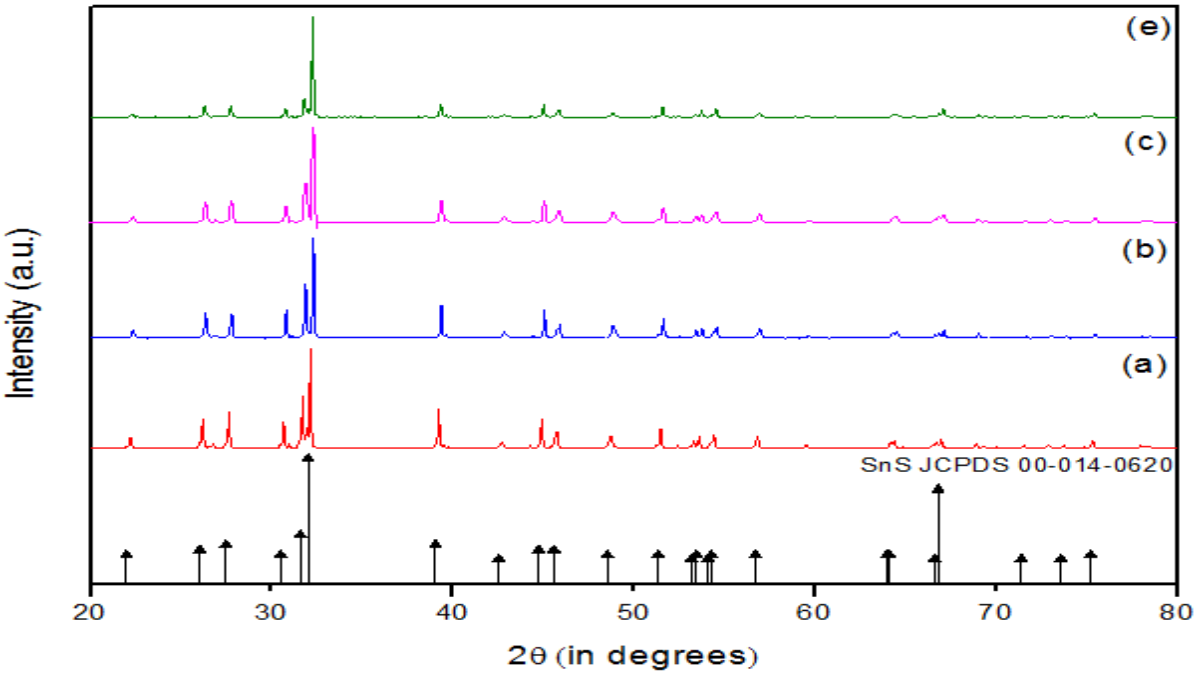

Figure 10: comparison of XRD patterns of materials synthesized by method 1 at 180^0C for different times of reaction; (a) at 12h, (b) at 14h, (c) at 16h, (d) at 18h.

Figure 9, figure 10 and table 2 do not show any changes in particle shape and elemental composition. i.e. Time variation does not affect the formation of SnS at 180^0C.

4.2.2 Method 2 optimization

In case of Method 2 where Na_2S was used as the Sulfur source, morphological changes in particles and decrease in Sulfur content were clearly observed with increase in reaction temperature (figure 11 and table 3). The major morphology obtained when reaction temperature was 120^0C, was nano-sized rods of SnS but an increase in reaction temperature causes increased tendency to form Tin rich nanoflakes. These Tin rich nanoflakes showed flower-like assembly at even more higher temperatures (At 180^0C, 200^0C). Comparison of their XRD patterns is evident to see these changes clearly (figure 12).

4.2.2.1 Temperature variation

FESEM Analysis:

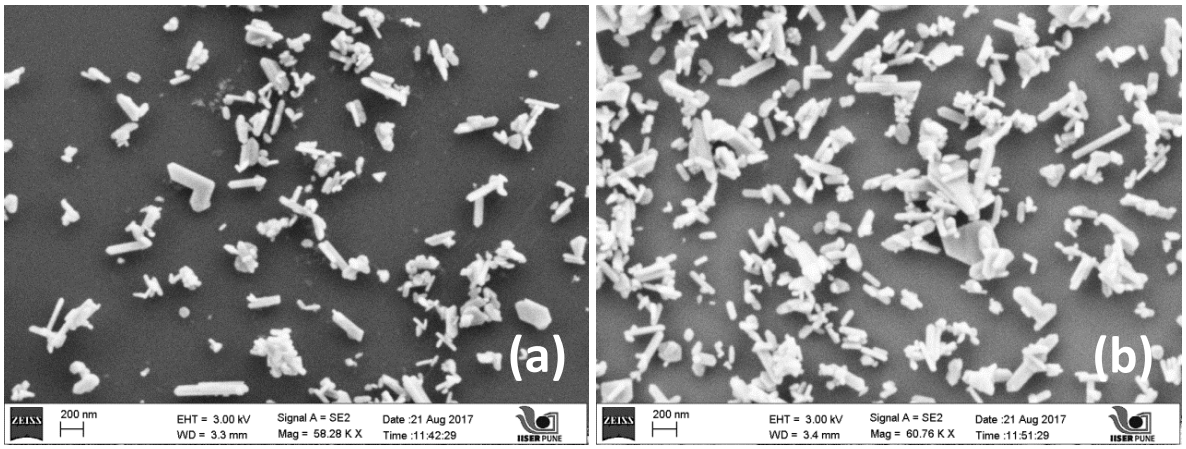

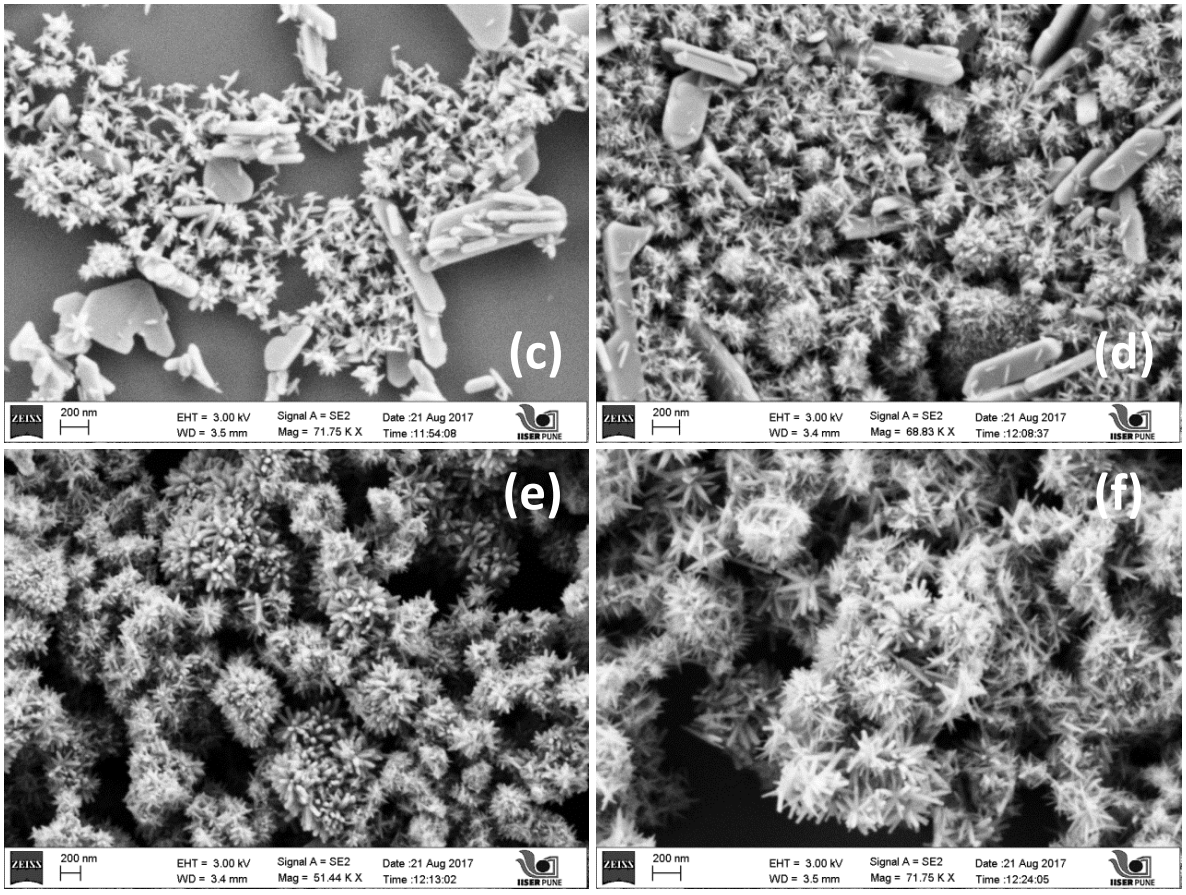

	Temperature	EDAX	
		Sn (%)	S (%)
(a)	120^{0}C	51.99	48.01
(b)	140^{0}C	53.11	46.89
(c)	160^{0}C	81.84	18.16
(d)	170^{0}C	93.47	6.53
(e)	180^{0}C	95.12	4.88
(f)	200^{0}C	95.2	4.8

Table 3

Figure 11: FESEM images (a-f) of major marphologies obtained by method 2 with reaction time fixed for 12 hours and reaction temperature (a) 120^{0}C, (b) 140^{0}C, (c) 160^{0}C, (d) 170^{0}C, (e) 180^{0}C, (f) 200^{0}C. Whereas ***Table 3*** shows Tin, Sulfur percentages of particles from EDAX analysis.

XRD analysis:

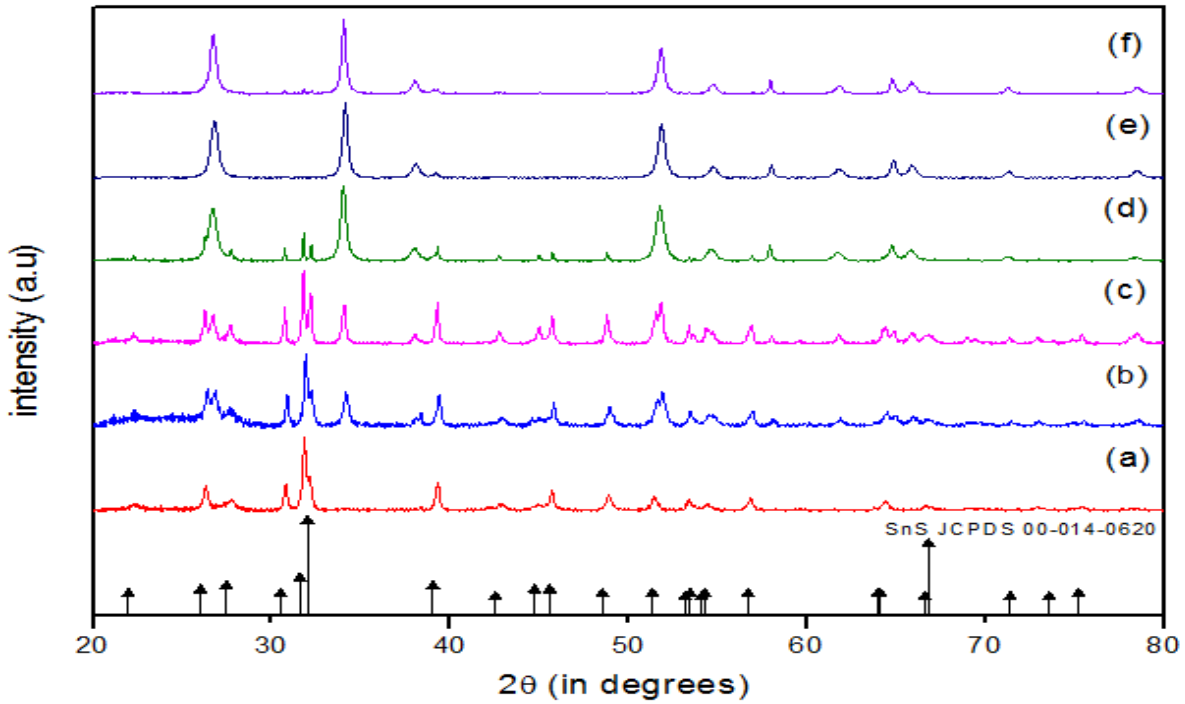

Figure 12 **:** comparison of XRD patterns of materials synthesized by method 2 at different temperatures for 12 hours; (a) at 120^0C, (b) at 140^0C, (c) at 160^0C, (d) at 170^0C, (e) at 180^0C, (f) at 200^0C.

Morphology of particles changes with increasing reaction temperature. At lower temperature (at 120^0C and 140^0C) most of the particles are rods of few nanometers in size. EDAX data show rods are nearly 1:1 in Sn to S ratio. At higher temperature (at 180^0C, 200^0C) uniform distribution of nanoflakes was observed. Thee nanoflakes look self-aggregated to form flower-like shape. They mostly consist of Tin and very less sulfur is present in them. In middle range of temperature (160^0C, 170^0C) a mixture of rods, nanoflakes and plates at some places were observed. Interestingly, These gradual changes/shift in morphology and elemental composition are reflected in the XRD patterns of these materials which support the observation that Sn content increases and sulfur content decreases with increase in temperature of reaction.

4.2.2.2 Time Variation

FESEM Analyis:

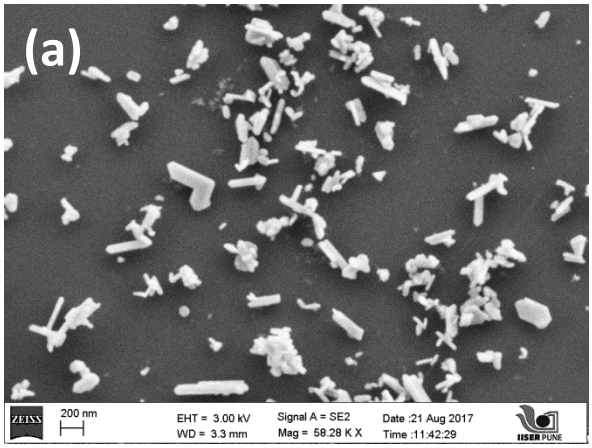

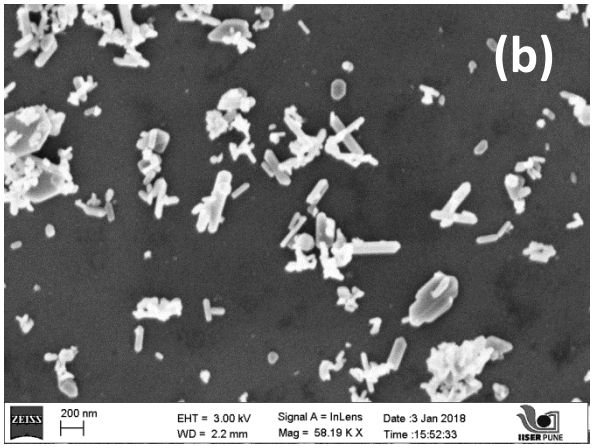

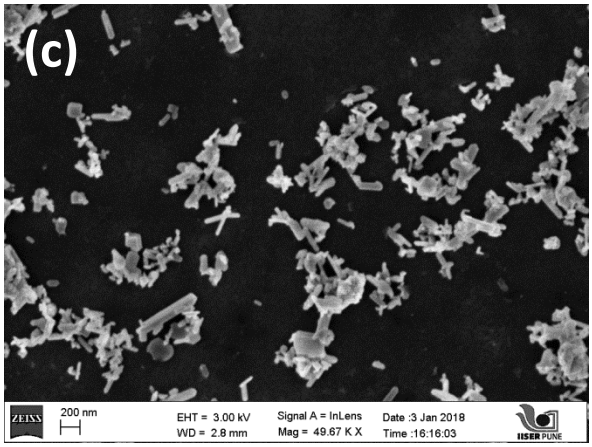

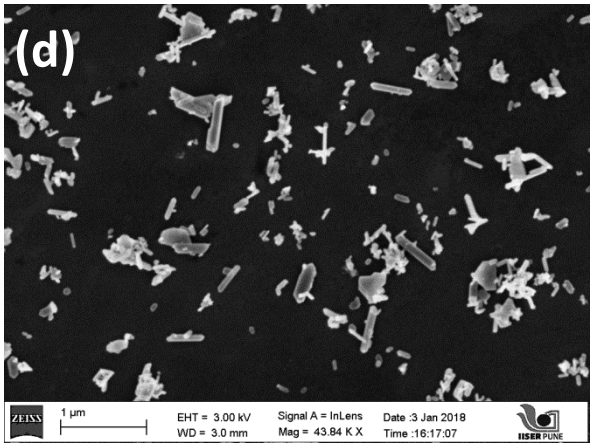

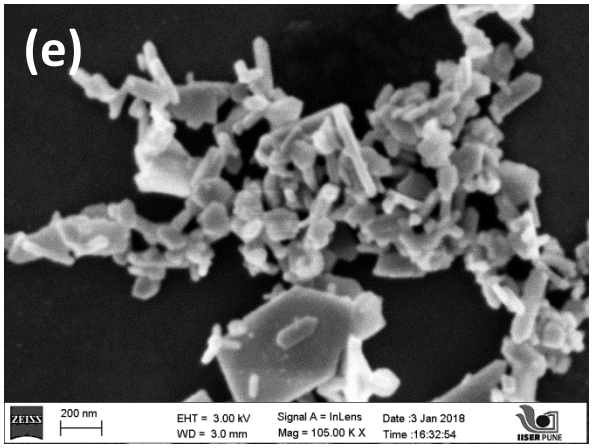

	Time	EDAX	
		Sn	S
(a)	12h	51.99	48.01
(b)	14h	47.41	52.59
(c)	16h	50.73	49.27
(d)	18h	45.9	54.1
(e)	20h	48.84	51.16

Table 4

Figure 13: FESEM images (a-e) of major morphologies obtained by method 2 with reaction temperature fixed at 120^0C and reaction time (a) 12 hours (b) 14 hours (c) 16 hours (d) 18 hours (e) 20 hours. Whereas ***Table 4*** shows Tin, Sulfur percentages of particles from EDAX analysis.

XRD Comparison:

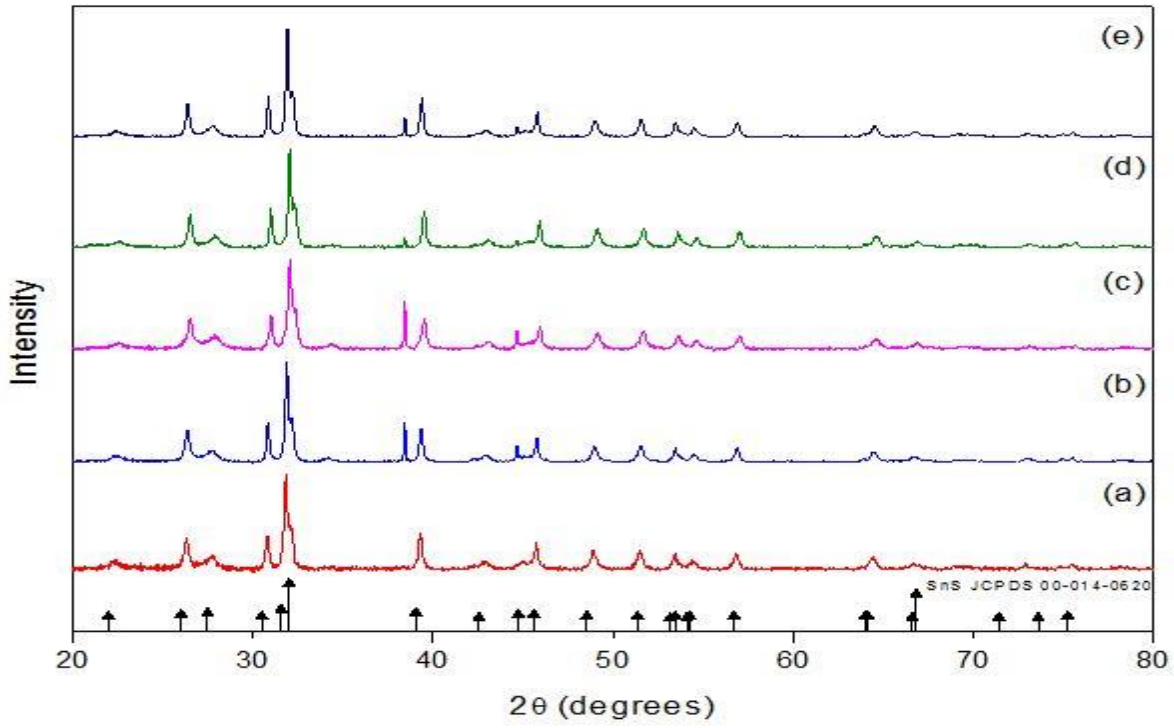

Figure 14**:** comparison of XRD patterns of materials synthesized by method 2 at 120^0C for (a) 12 hours (b) 14 hours (c) 16 hours (d) 18 hours (e) 20 hours.

Changing reaction time did not affect the formation of nano-sized rods at 120^0C. FESEM images from figure 13 show increasing size distribution of rods instead of changes in morphology. EDAX values of both Sn and S were fluctuating around 50%. Also, XRD patterns of these materials show consistent pattern of SnS with slightly broad peaks which indicates that rod size is in nanoscale.

After completion of optimization of both methods, Method 1 needed no changes. SnS was formed by method 1 with plate-like morphology of particles. Particles of SnS were few micrometer in size, quite large, and this could be inferred from the sharp peaks which appeared in its XRD pattern. Method 2, on the other hand, needs a slight change. The temperature of reaction which initially was 160^0C is now changed to 120^0C in order to get only SnS as product. Interestingly, particle size, in this case, is of few nanometers as it can be seen in the XRD pattern that peaks have became slightly broader.

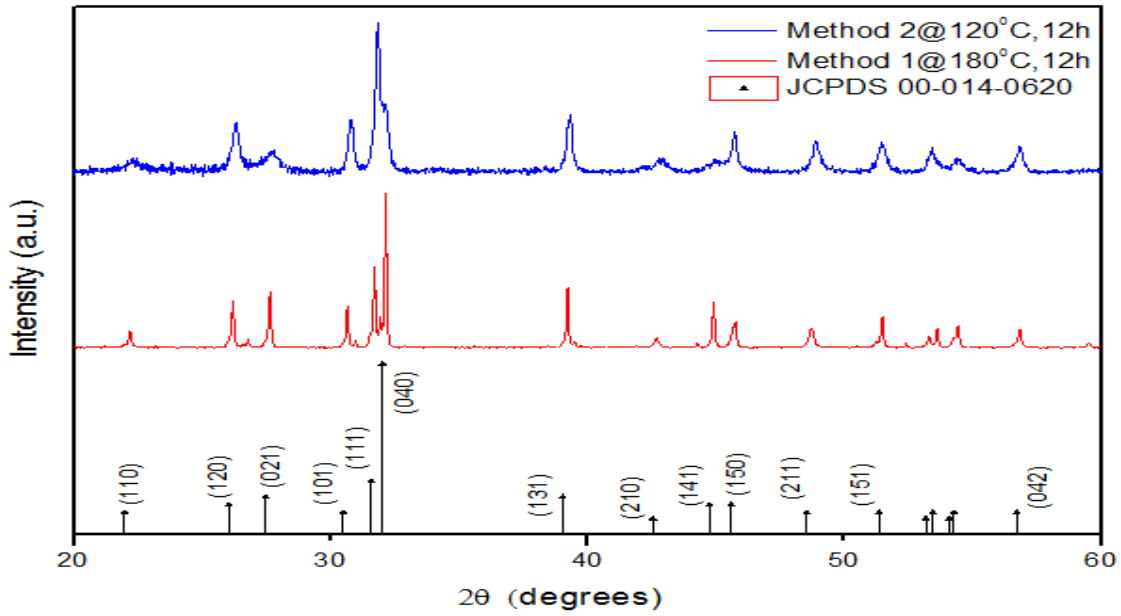

Figure 15: comparison of XRD patterns of SnS synthesized by method 1 and method 2.

Thus updated Method 1 and Method 2 after optimization are-

Method 1

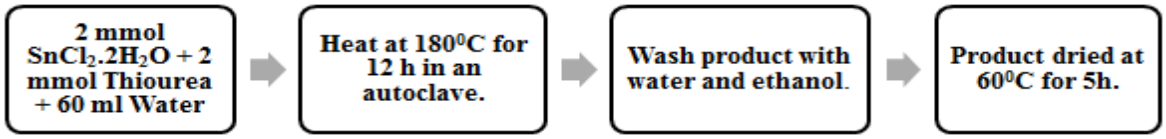

Method 2

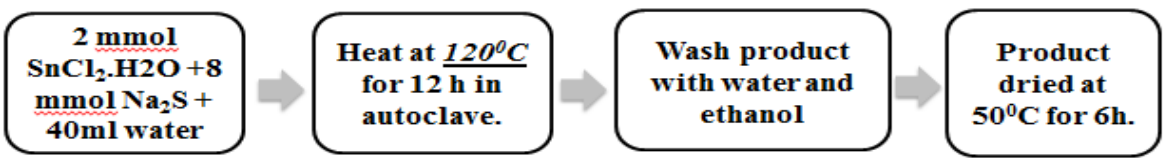

Figure 16: updated method 1 and method 2

4.3 Thermal Analysis of material

The materials which were synthesized by updated method 1 and method 2 will be checked for thermoelectrics. Thus it was important to understand thermal behaviour of the materials. Thermogravimetric Analysis (TGA) and Differential scanning calorimetry (DSC) were carried out.

TGA of SnS synthesized by method1:

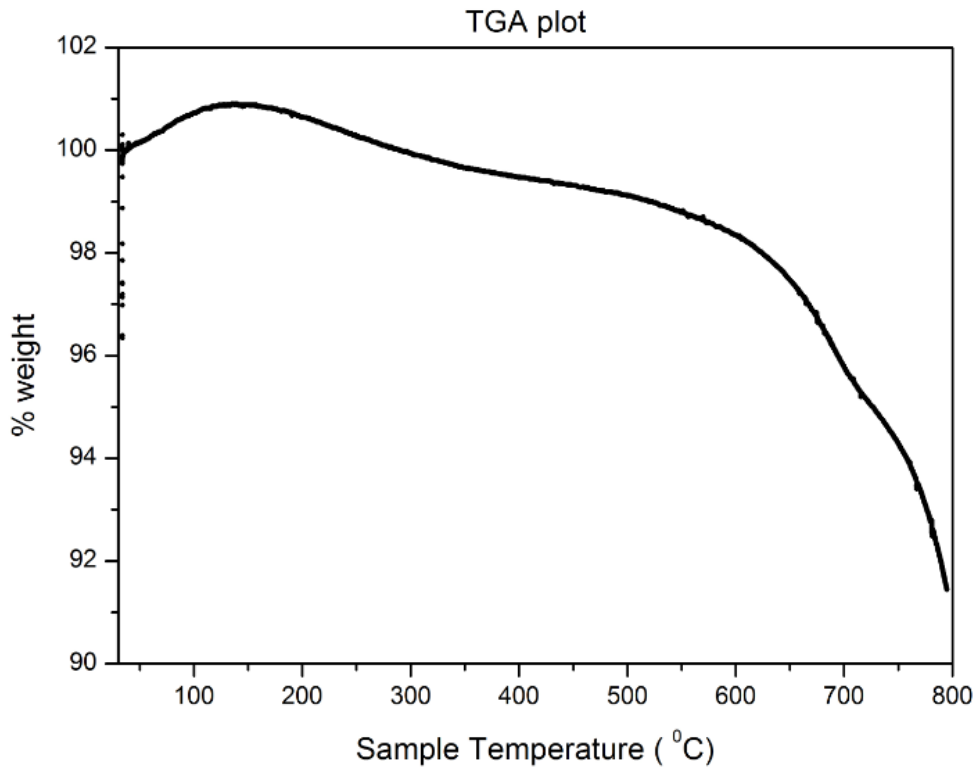

Figure 17: a plot of thermogravimetric analysis of SnS synthesized by method 1.

TGA of material was done under N_2 atmosphere from room temperature to 800^0C. Material was quite stable till 500^0C as only 1% weight loss was observed in TGA plot.

DSC of material synthesized by method 1:

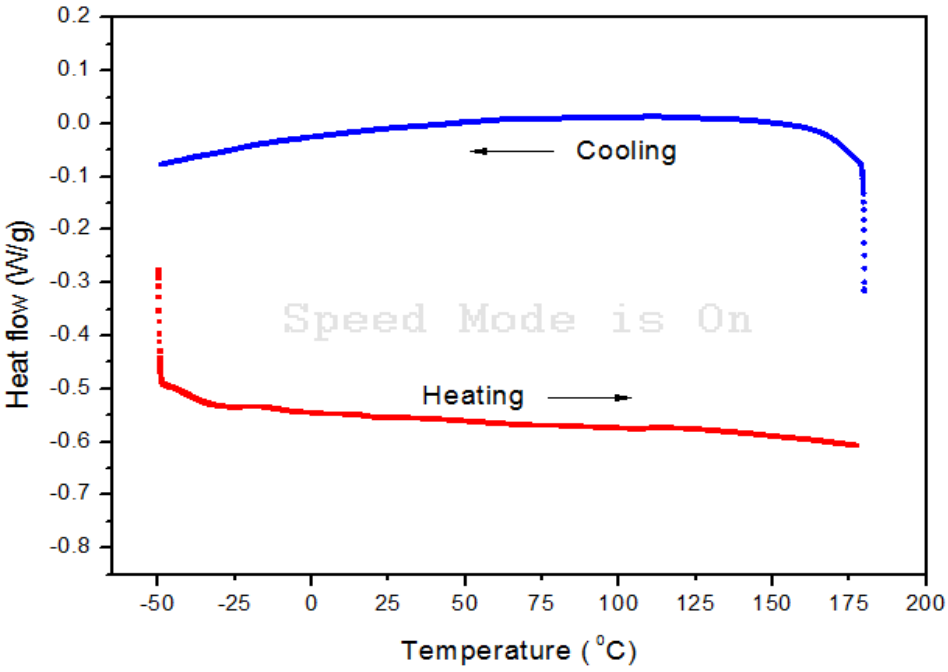

Figure 18: DSC thermogram of SnS synthesized by method 1.

DSC was done up to 180^{0}C. No significant calorimetric changes were observed in the thermogram.

TGA of SnS synthesized by method2:

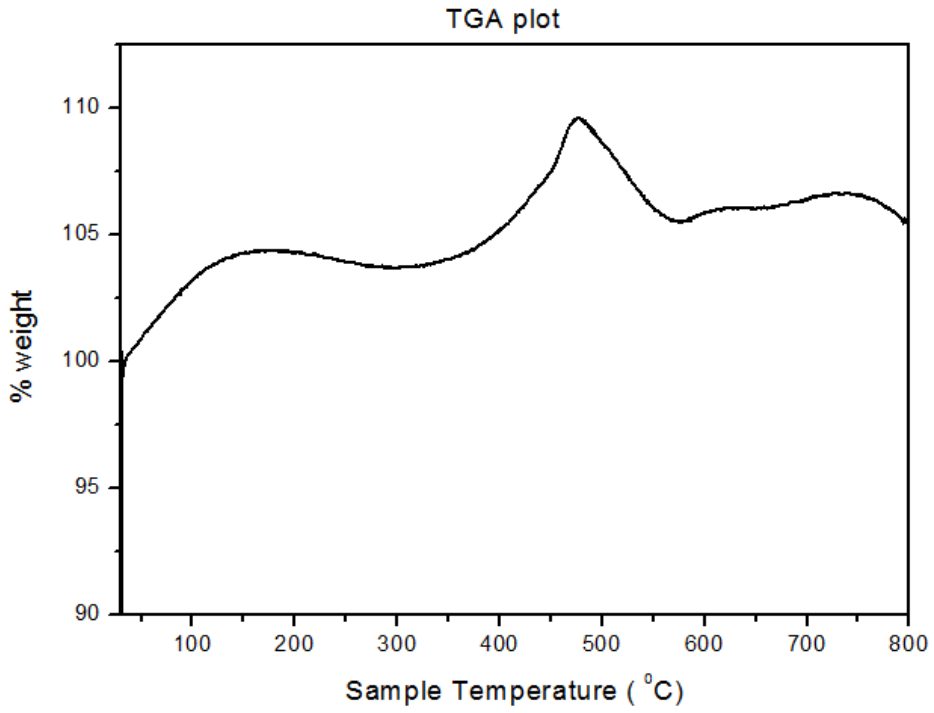

Figure 19: a plot of thermogravimetric analysis of SnS nanorods synthesized by method 2

TGA plot of SnS nanorods does not show any weight loss. TGA was done under N_2 atmosphere. (so one can think of the possibility of the nitrogen getting adsorbed on the surface of nanorods.)

DSC of material synthesized by method 1:

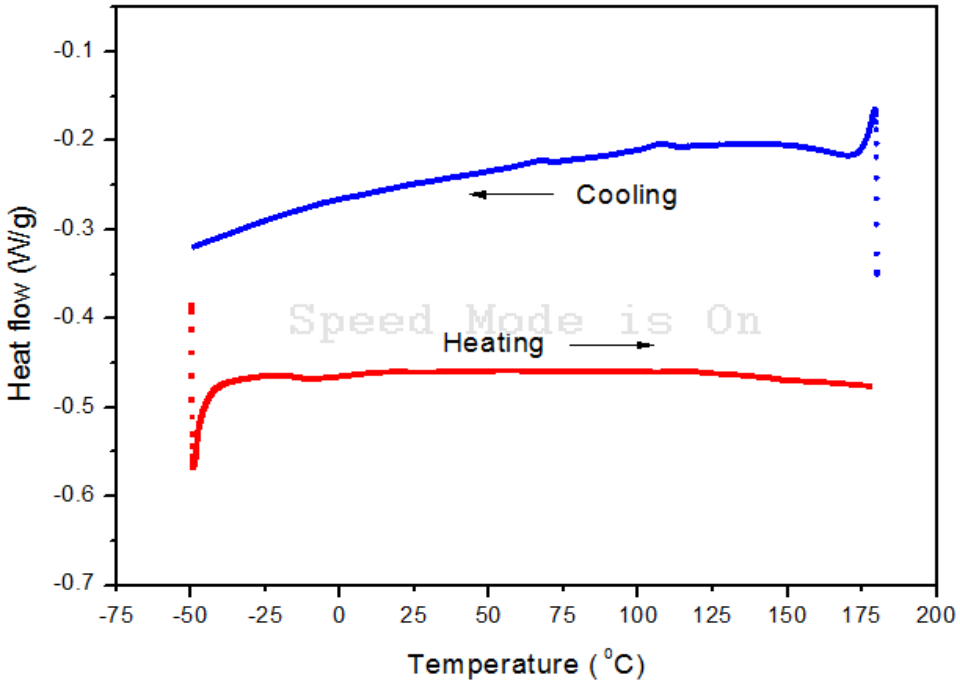

Figure 20: DSC thermogram of SnS nanorods synthesized by method 2.

No drastic calorimetric changes were seen in the DSC thermogram except two small humps during cooling.

4.4 Pelletisation of material.

To measure Thermal diffusivity of the material, the Laser Flash Apparatus (LFA) requires a sintered pellet of material which is 13mm in diameter and around 2mm thick.

Thus several syntheses were performed to scale up the material, initially by method 1. Once enough quantity (around 1gm) of material was synthesized, the powdered material was then pressed in KBr press using 13mm die under a pressure of approximately 8.5 tonnes for 5 minutes.

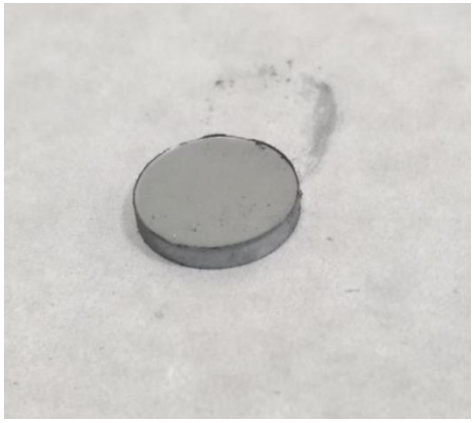

Figure 21: an SnS pellet synthesized by method 1.

The pellet was sintered at 300^0C for 12 hours in a tube furnace under Nitrogen atmosphere. Then FESEM, EDAX and XRD of pellet surface were carried out to see the surface after sintering.

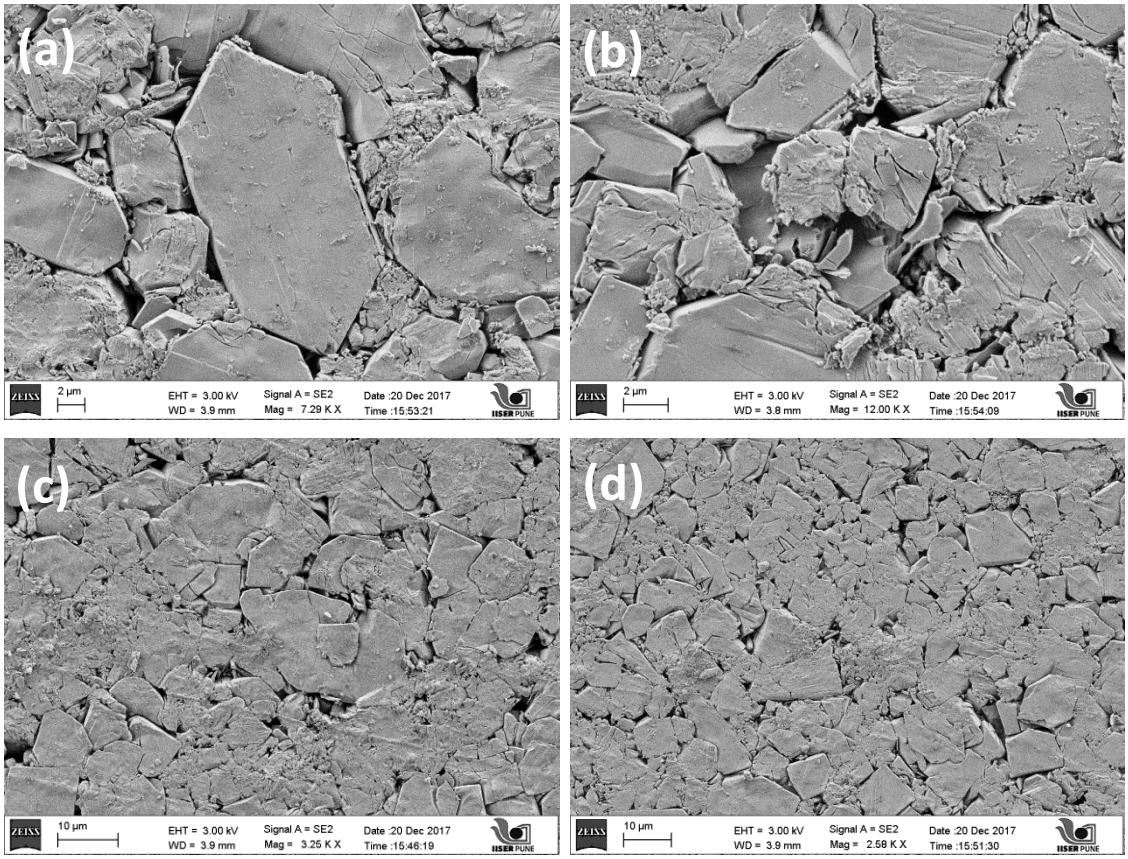

Figure 22: (a-d) FESEM images of pellet surface

Element	Weight%	Atomic%
S K	20.91	49.46
Sn L	79.09	50.54
Totals	100.00	

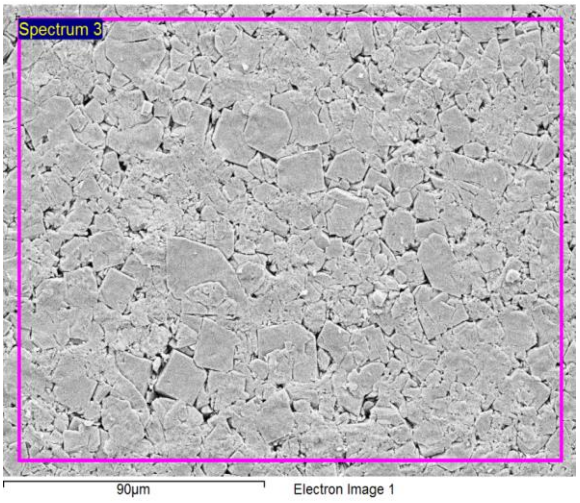

Figure 23: EDAX analysis of pellet surface

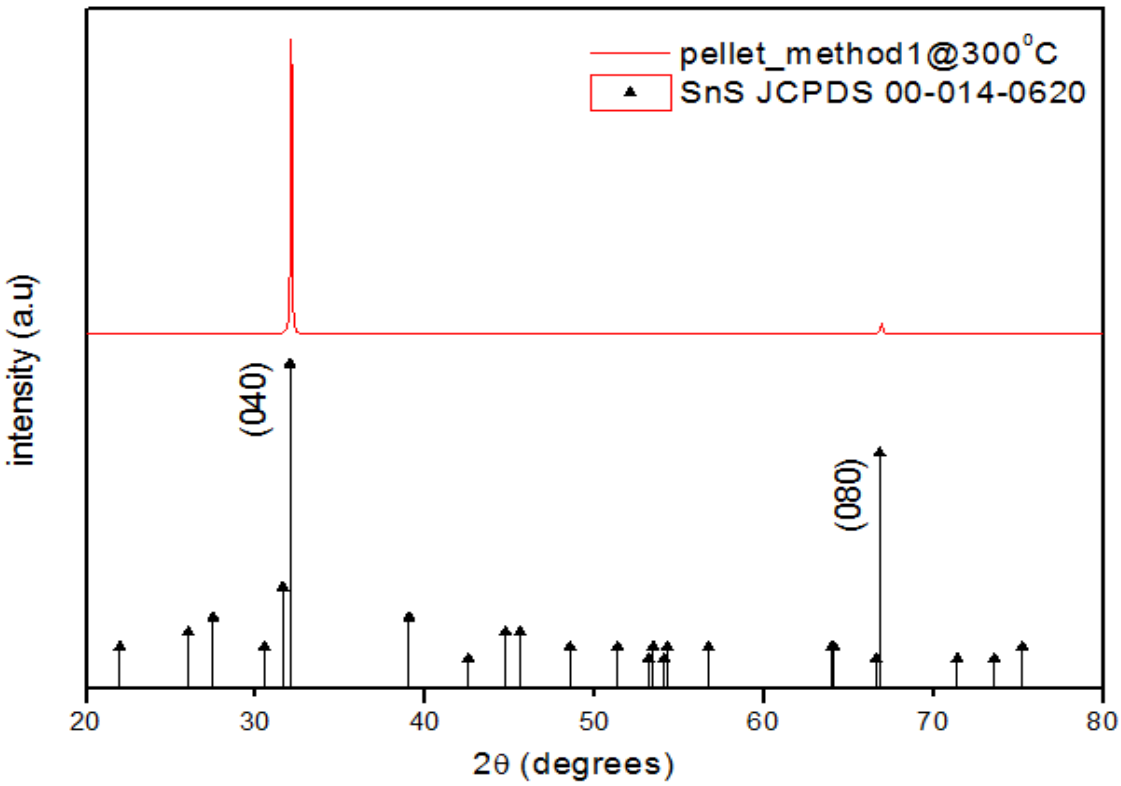

Figure 24: X-ray diffraction pattern of SnS pellet sintered at 300^0C

Considering the thermal stability of SnS synthesized by method 1 (figure17), we decided to sinter the pellet again, but this time at a temperature higher than previous, at 500^0C. (LFA measurement data would be more reliable if temperature range is high).

Thus under the same condition except temperature being 500^0C, pellet was sintered again. Newly sintered pellet was examined by doing X-ray diffraction. It was found that the entire pellet was oxidized. (An error might have occurred while sealing the furnace so that N_2 atmosphere could not be maintained.)

Following figures 25 and 26 show pellet sintered at 500^0C is oxidized and the new peaks that arose in the XRD belong to SnO_2. Figure 25 compares XRD of pellet sintered at 300^0C with XRD of same pellet sintered at 500^0C. Figure 26 confirms the new peaks belong to SnO_2 by comparing it with SnO_2 JCPDS.

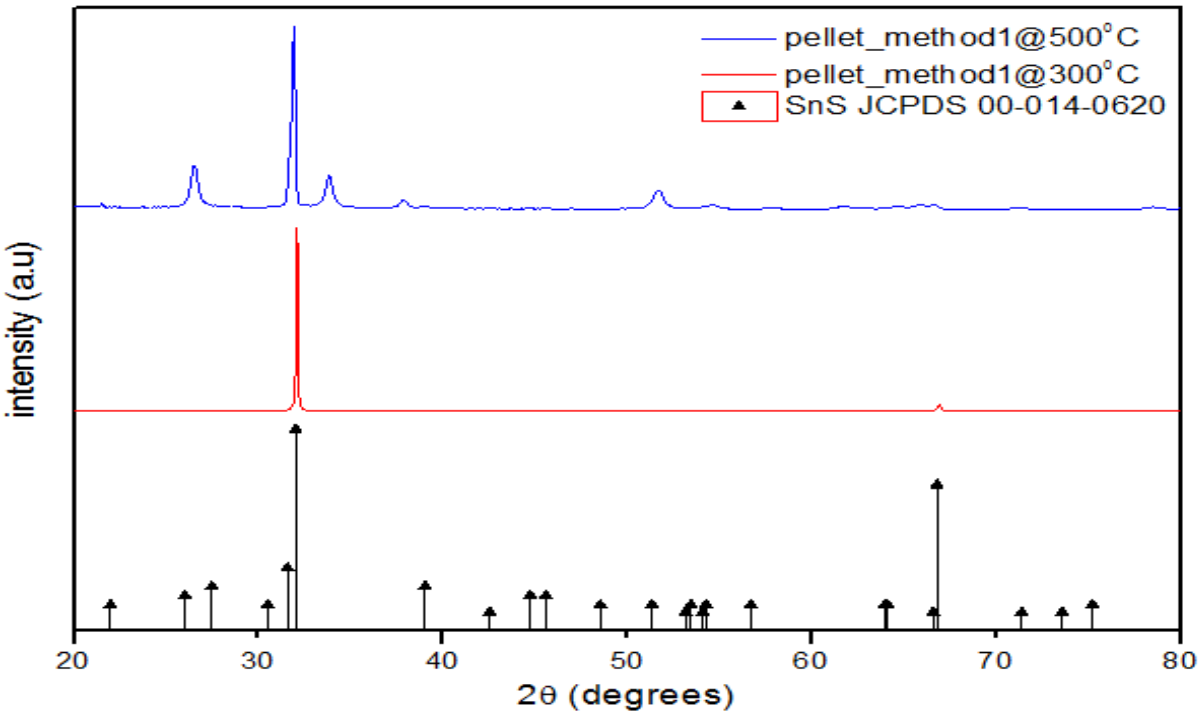

Figure 25: comparison of pellet XRD after sintering at different temperatures.

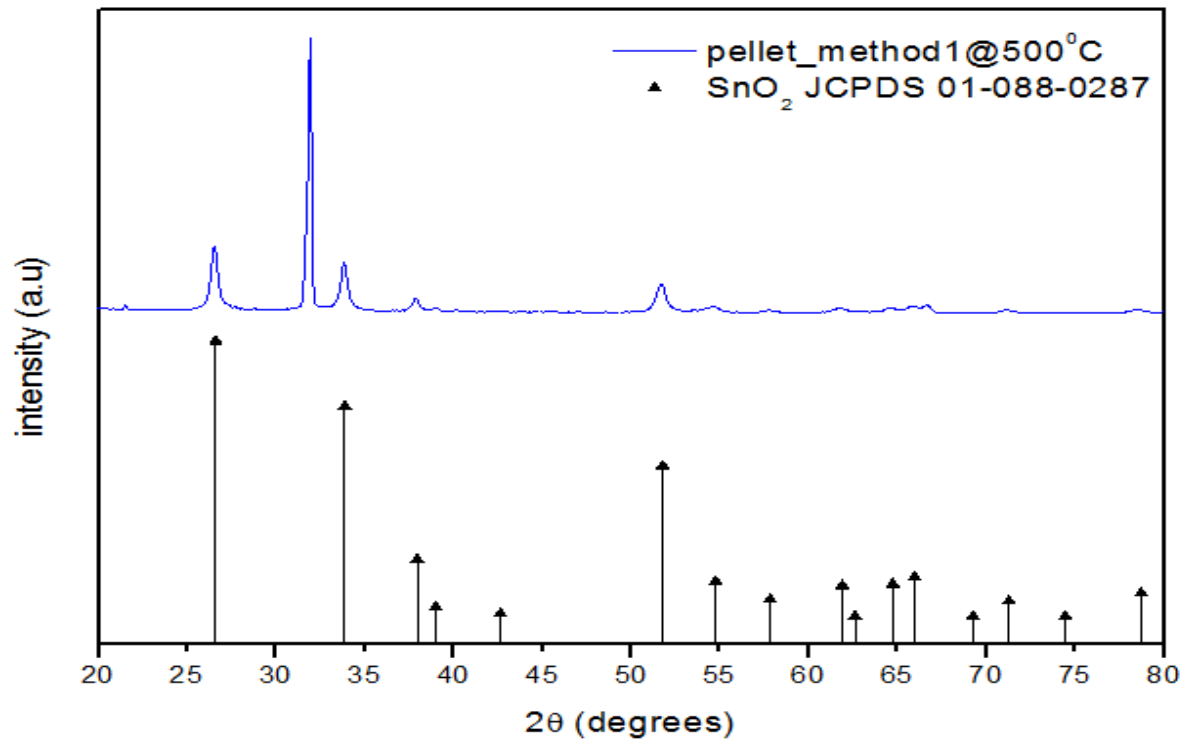

Figure 26: comparison of XRD pattern of pellet sintered at 500^0C with SnO_2 JCPDS.

Since the first pellet was oxidized, another set of syntheses were performed by method 1 to scale up the material. After completing scale-up of method 1 SnS, method 2 SnS material (nanorods) was also scaled up for pelletizing. Method 1 SnS was pelletized in the same way as previously done, by applying around 8.5 tonnes of pressure for 5 minutes using KBr press. Similarly, method 2 SnS was also pelletized.

This time sintering was done at a different place than previous. Both the pellets were kept in a crucible at some distance apart. Sintering was done in the tube furnace (different than the previous one) at 500^0C for 12 hours. An inert atmosphere of Argon was supplied this time.

Inert atmosphere could not be maintained properly this time too. Both the pellets ended up being oxidized. Following XRD data shows that the pellets were oxidized.

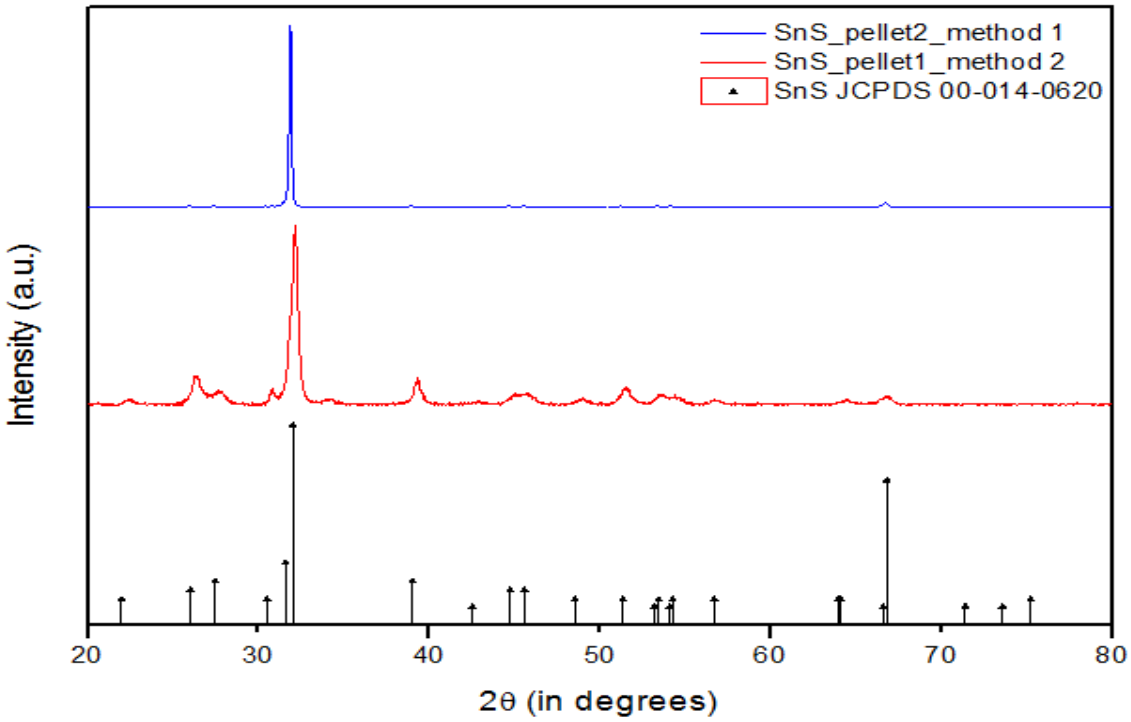

Figure 27: newly made pellets of method 1 SnS and method 2 SnS(nanorods)

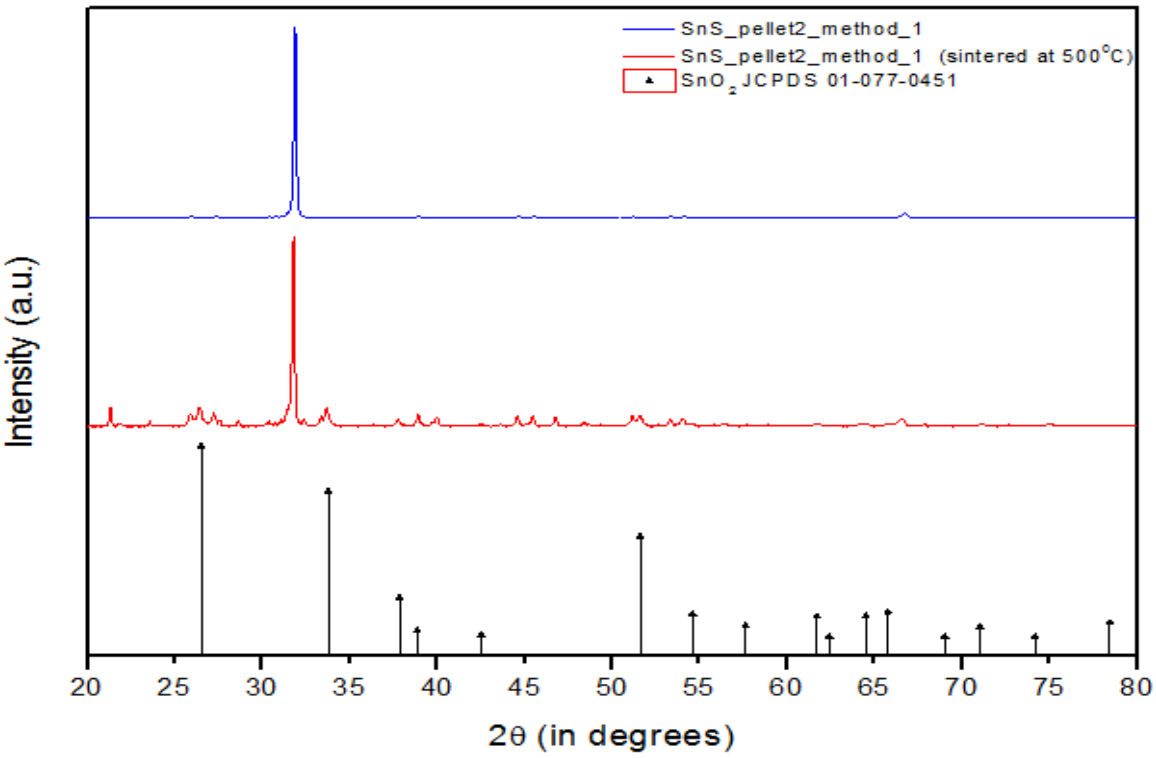

Figure 28: comparison of XRD pattern of newly made method 1 SnS pellet to the XRD pattern of same pellet after sintering at 500^0C.

Some new peaks arose after sintering. The SnO2 JCPDS peaks match with their positions.

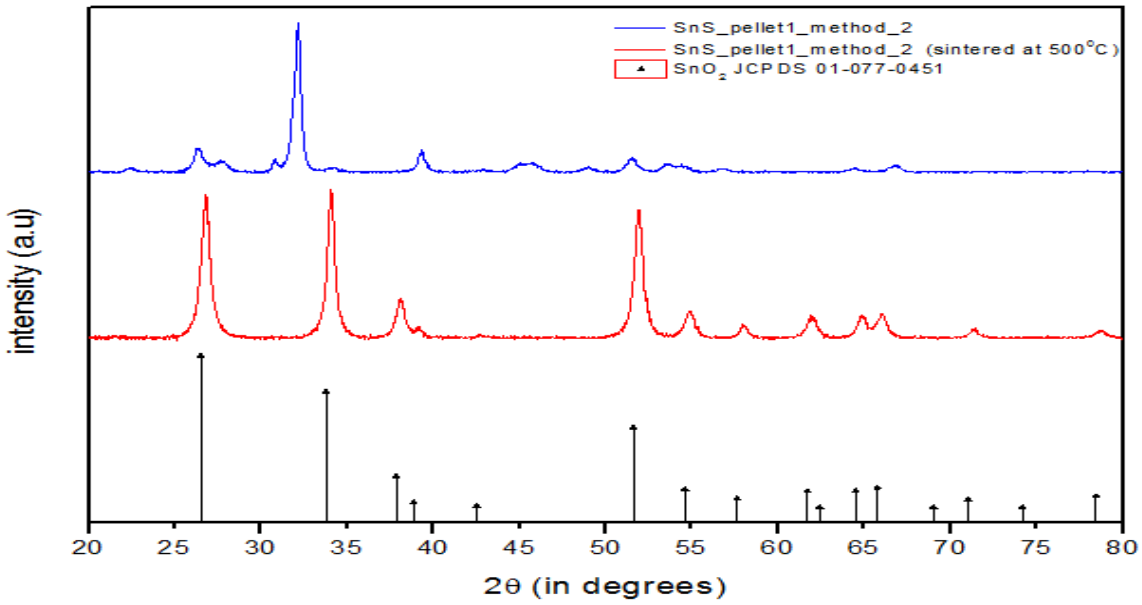

Figure 29: comparison of XRD pattern of new SnS pellet made by method 2 to the XRD pattern of same pellet after sintering at 500^0C.JCPDS confirms oxidation of it.

The next step after successful sintering of pellet is to measure the thermal diffusivity of material in Laser Flash Apparatus. Then cutting the pellet into a rectangular rod of length 12 mm having width and height of 2 mm for the purpose of Seebeck coefficient and resistivity measurements in LSR (Linseis – Seeback and Electrical Resistivity Unit)

But all three pellets were oxidized. Thus we could not perform thermoelectric measurements.

5. Conclusions

- SnS was successfully synthesized by both methods (method 1 and method 2) using green approach.
- Both methods were successfully optimized to give particles of specific morphology and composition.
- Sintering of pellets is necessary without oxidation and required for thermoelectrics which needs to be achieved. Further work is going on.

6. References

1. Zhang, X. & Zhao, L. D. Thermoelectric materials: Energy conversion between heat and electricity. *J. Mater.* **1,** 92–105 (2015).

2. Zhao, L.-D., Dravid, V. P. & Kanatzidis, M. G. The panoscopic approach to high performance thermoelectrics. *Energy Environ. Sci.* **7,** 251–268 (2014).

3. Zhao, L.-D. *et al.* Ultralow thermal conductivity and high thermoelectric figure of merit in SnSe crystals. *Nature* **508,** 373–377 (2014).

4. Tan, Q., Zhao, L., Li, J., Wu, C. & Wei, T. Thermoelectrics with earth abundant elements : low thermal conductivity and high thermopower in. *J. Mater. Chem. A Mater. energy Sustain.* **2,** 17302–17306 (2014).

5. Wang, G. *et al.* Two-dimensional SnS_2 @PANI nanoplates with high capacity and excellent stability for lithium-ion batteries. *J. Mater. Chem. A* ***3,*** **36**59–3666 (2015)

6. Shi, W. *et al.* Hydrothermal growth and gas sensing property of flower-shaped SnS_2 nanostructures. *Nanotechnology* **17,** 2918–2924 (2006).

7. Zhai, C., Du, N. & Yang, H. Z. D. Large-scale synthesis of ultrathin hexagonal tin disulfidenanosheets with highly reversible lithium storage. *Chem. Commun.* **47,** 1270–1272 (2011).

8. Kulkarni, S. K. *Nanotechnology : Principles and Practices*.